# Glass encapsulation of molecular-doped epitaxial graphene for quantum resistance metrology

OPEN ACCESS
IOP Publishing
Measurement Science and Technology
Meas. Sci. Technol. **33** (2022) 115019 (8pp)
https://doi.org/10.1088/1361-6501/ac8222

# Glass encapsulation of molecular-doped epitaxial graphene for quantum resistance metrology

**Jaesung Park*, Kyung-Geun Lim and Dong-Hun Chae***

Korea Research Institute of Standards and Science, Daejeon 34113, Republic of Korea

E-mail: jspark99@kriss.re.kr and dhchae@kriss.re.kr

Received 15 March 2022, revised 9 July 2022
Accepted for publication 18 July 2022
Published 25 August 2022

**Abstract**

The large Landau energy spacing, stemming from the linear energy-momentum dispersion of quasi-particles in graphene, allows an efficient realization of the quantum Hall effect at a small density of charge carriers. Promising scalable epitaxial graphene on silicon carbide (SiC), however, requires molecular doping, which is generally unstable under ambient conditions, to compensate for electron transfer from the SiC substrate. Here, we employed classical glass encapsulation common in organic electronics to passivate molecular-doped epitaxial graphene against water and oxygen molecules in air. We have investigated the stability of Hall quantization in a glass-encapsulated device for almost 1 year. The Hall quantization is maintained above a threshold magnetic field within 2 n$\Omega$ $\Omega^{-1}$ smaller than the measurement uncertainty of 3.5 n$\Omega$ $\Omega^{-1}$ through multiple thermal cycles for almost 1 year, while the ordinary unencapsulated device in air distinctly shows a relative deviation larger than 0.05% from the nominal quantized Hall resistance in 1 month.

Supplementary material for this article is available online

Keywords: quantized Hall resistance, graphene, stability, encapsulation

(Some figures may appear in colour only in the online journal)

## 1. Introduction

The quantum Hall effect [1] plays a key role in realizing the resistance standard which is directly traceable to the fixed values of the fundamental constants in the framework of the new International System of Units (SI) that became effective in 2019 [2, 3]. Many metrology institutes realize the SI Ohm based on the quantized Hall resistance (QHR) of $h/\left(2e^2\right)$ for filling factor 2 in the GaAs/AlGaAs heterostructure. This realization, however, demands temperatures below 1.5 K and a magnetic field of approximately 10 T due to the small Landau energy spacing in the material [4]. The observed quantum Hall effect in graphene is characteristically distinct from that in semiconductors. The emergent quantum Hall effect at relatively high temperatures and low magnetic fields is attributed to the large energy spacing between Landau levels. It arises from massless quasi-particles following the linear energy-momentum dispersion in graphene [5–7]. This difference triggered the research and development of graphene for metrology applications from a practical point of view.

Since a metrological demonstration [8] of Hall quantization with graphene grown on silicon carbide (SiC), epitaxial graphene has been employed to demonstrate a QHR under relaxed experimental conditions with metrological accuracy

* Authors to whom any correspondence should be addressed.



 

[9–13]. Additionally, epitaxial graphene on SiC with a small carrier density may provide a scalable platform for quantum resistance metrology [14, 15]. Moreover, graphene has been under investigation for an impedance quantum standard which is directly traceable to the Planck constant, $h$, and the elementary charge, $e$, of the SI [16–18]. In practice, however, its long-term stability under ambient conditions is still lacking for resistance or impedance quantum metrology. Epitaxial graphene has a buffer layer at the interface between graphene and the SiC substrate. In general, donor states in the buffer layer lead to high electron doping in graphene of approximately $10^{12}$–$10^{13}$ cm$^{-2}$ [19]. Therefore, hole doping is required to reduce the carrier density to approximately $10^{11}$ cm$^{-2}$ or below to fulfill the filling factor condition for an emergent quantum Hall effect at an achievable magnetic field in laboratories. Various doping methods based on organic molecules have been devised to induce strong hole doping on epitaxial graphene [20–23]. Organic materials are, however, generally vulnerable to moisture and oxygen in the air [24, 25]. Thus, epitaxial graphene needs a protective layer for stability, as found in organic electronic devices [26]. Moreover, it has been reported that carbon clusters are absorbed on epitaxial graphene when exposed to air [27]. This may deteriorate the transport property of epitaxial graphene in the quantum Hall regime. Encapsulation methods have been developed for epitaxial graphene using parylene [28] or amorphous boron nitride [29, 30], which have turned out to be unsuitable for metrological applications. Recently, the functionalization of epitaxial graphene with chromium tricarbonyl [31, 32] was employed to reversibly adjust the carrier density without an electric gate [33]. Although this method seems to be applicable to the realization of QHR standards, the adsorption of water and oxygen molecules on epitaxial graphene needs to be controlled carefully by heating. The consequent QHR needs to be evaluated frequently. On the other hand, He and his collaborators stored graphene devices under an inert atmosphere in a glove box to minimize air exposure [34]. Recently, an interlaboratory comparison was performed with a delivery container overpressurized by an inert gas [35]. However, degradation cannot be avoided even during short-term air exposure.

Here, we examine the stability of glass-encapsulated molecular-doped epitaxial graphene for quantum resistance metrology. Glass lids are commonly employed for the passivation of organic electronic devices against water and oxygen molecules at room temperature [36]. Until now, however, there has not been a test of whether this classical glass encapsulation is applicable to molecular-doped epitaxial graphene for quantum resistance metrology at cryogenic temperatures through multiple thermal cycles. Here, we exposed a glass-encapsulated graphene device to ambient conditions for almost 1 year. Hall quantization was monitored with metrological accuracy over time. The robustness test also included exposure to 90% humidity for 24 h during the period as an acceleration experiment. Experimental results show that the QHR realized in the glass-encapsulated device is maintained within a measurement uncertainty of a few parts in $10^9$ during the investigated period. This shows that this simple method has the potential to be employed for graphene-based quantum resistance metrology.

## 2. Experimental methods

### 2.1. Device fabrication

The graphene device was fabricated in a similar way as in a previous report [13]. Quality graphene was grown on SiC at 1600 °C under an argon atmosphere at a pressure of approximately 100 kPa [37] with the polymer-assisted sublimation method [11]. A modified graphite susceptor with a small gap was employed for slow sublimation of silicon atoms to avoid step bunching of the terrace structure. To evaluate the quality of the as-grown graphene, we employed atomic force microscopy (AFM) and scanning probe Raman spectroscopy. The channel and metal contacts were patterned with electron-beam lithography and reactive ion etching. The device channel was aligned with the direction of the terrace of the epitaxial graphene probed with AFM. Palladium (Pd)/gold (Au) (20 nm/40 nm) was deposited for contact because Pd leads to a small contact resistance [38]. The graphene device was then annealed to remove the organic residues from the fabrication process in vacuum at 500 °C for 30 min. The length and width of the graphene channel were 440 μm and 100 μm, respectively. The contact resistance determined in a three-probe configuration [39] at the quantum Hall state was approximately 1 Ω.

We followed a molecular doping method [23] to compensate for the electron transfer from the SiC substrate. Trilayers of a polymer spacer, a polymer mixture with 2,3,5,6-tetrafluoro-tetracyano-quino-dimethane (F4-TCNQ) as the hole dopant, and the same polymer spacer were spin-coated to reduce the carrier density. Poly(methyl methacrylate) (PMMA)-based copolymer (MMA (8.5) MAA) EL6 (6% in ethyl lactate) was employed for the polymer spacer. The polymer mixture was made by mixing F4-TCNQ (25 mg), anisole (3 ml), and PMMA A6 (6 ml, 6% PMMA solution in anisole). Each layer was spin-coated at 6000 rotations per minute for 1 min. The first polymer spacer (the second polymer mixture and the third polymer spacer) was baked on a hot plate at 160 °C for 5 min (1 min). Finally, the device was annealed at 160 °C for 2 min for diffusion of the hole dopants toward graphene. All doping processes were performed in a glove box to minimize exposure to moisture and oxygen.

To encapsulate the graphene device against air, we designed a glass lid with a cavity at the center as illustrated in figure 1(a). Soda-lime glass was employed for the lid. The dimensions of the glass lid and cavity were 4.2 mm × 4.2 mm × 1.1 mm and 2.2 mm × 2.2 mm × 0.8 mm, respectively. Machine milling was applied to create the cavity. The glass lid was glued on top of the device using epoxy [40] in a nitrogen atmosphere in a glove box, while the bonding pads were located outside the glass lid for wiring on a chip carrier. We adjusted the amount of epoxy on the glass lid with a scalpel to form a thin and flat epoxy adhesive. Two-component epoxy may introduce a chemical byproduct that may dope graphene. A

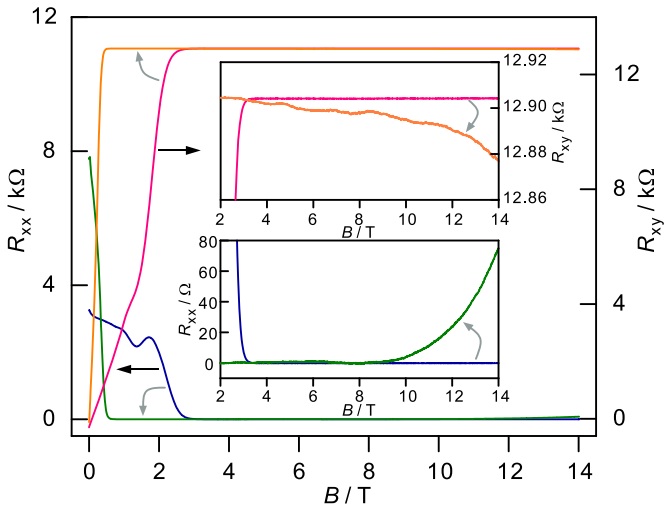


**Figure 1.** Magnetoresistance change in the graphene device stored in air in the laboratory for 1 month. Insets show the transverse (upper) and longitudinal (lower) magnetoresistances in the magnified ranges.

control experiment showed that the Hall slope of two consecutive magnetoresistance measurements before and after glass encapsulation does not change significantly. This indicates that the mentioned doping is not significant on a short timescale (see figure S1 in supplementary material).

### 2.2. Experimental setup and uncertainty budget

To perform magnetotransport measurements and precision Hall resistance measurements, graphene devices were loaded in a cold-finger-type cryostat with a 14 T superconducting magnet and a base temperature of 2 K. For precision resistance measurement, the QHR in the graphene device was compared with a precalibrated 100 Ω resistance reference using a cryogenic current comparator (CCC) resistance bridge [41]. The numbers of turns for the primary and secondary coils were selected to make the turn ratio close to the nominal resistance ratio of $R_K/2$ to 100 Ω, where $R_K = \frac{h}{e^2}$. Here, we used 4001 and 31 for the primary and secondary coils, respectively. We typically drive a current of 38.74 μA (5 mA) through a graphene device (the resistance reference), leading to a Hall voltage (voltage drop) of 0.5 V. To minimize the offset of the bridge voltage difference and its temporal drift, the polarity of the applied currents was reversed every 10 s. For each polarity, 200 data points were acquired. The first half of the acquired data points was ignored to avoid transient behavior after the current reversal. A typical measurement time of the Hall quantization was approximately 16 min.

Table 1 summarizes the contributions to the uncertainty budget for a typical measurement of QHR with the CCC via the resistance reference. The overall expanded measurement uncertainty ($k = 2$) at the 95% confidence level is approximately 3.5 nΩ $\Omega^{-1}$. The uncertainty of the 100 Ω resistance reference, precalibrated by a GaAs QHR standard [42], is approximately 1 nΩ $\Omega^{-1}$. An electric insulation of 10 TΩ results in an uncertainty of approximately 0.8 nΩ $\Omega^{-1}$. Another

**Table 1.** Uncertainty budget for a typical $R_{xy}$ measurement with the CCC resistance bridge.

| Contribution | Uncertainty (nΩ $\Omega^{-1}$) |
|---|---|
| Resistance reference | 1.0 |
| Electric insulation | 0.8 |
| Winding ratio error | 0.6 |
| SQUID resolution | 0.1 |
| Miscellaneous | $< 0.1$ |
| $\Delta U$ (type A) | 1.0 |
| Expanded measurement uncertainty ($k = 2$) | 3.5 |

significant contribution comes from the winding ratio error. Although the winding ratio error test showed an uncertainty of approximately a few parts in $10^{10}$, we conservatively assumed an error of 1 nΩ $\Omega^{-1}$. This leads to a value of 0.6 nΩ $\Omega^{-1}$ when the rectangular distribution is taken into account. The flux resolution limit of the employed superconducting quantum interference device (SQUID) also contributes to the uncertainty. The flux via the 31 turn coil induced by the driving current of 5 mA through the 100 Ω resistance reference is determined by the flux linkage [43] of 11 μA · turns/$\phi_o$ to be approximately 14 100 $\phi_o$. Here, $\phi_o$ is the quantum of the flux ($\frac{h}{2e}$). There is some evidence from ratio error tests on CCCs that rectification of noise can cause flux errors at the level of 1 μ$\phi_o$ in SQUIDs similar to the one used in this study [41]. We therefore assign an uncertainty of 1 μ$\phi_o$ to the SQUID output, and the corresponding flux error becomes1 μ$\phi_o$/14 100 $\phi_o$. When the rectangular distribution is considered, the relative uncertainty is close to 0.1 nΩ $\Omega^{-1}$. Other minor uncertainties include voltage measurement error of the nanovoltmeter in the bridge and an error from the employed auxiliary current source, which are smaller than 0.1 nΩ $\Omega^{-1}$. The statistical type-A is typically close to 1 nΩ $\Omega^{-1}$. The Allan deviation of the bridge voltage difference shows that the uncorrelated white noise is predominant for at least 1000 s sampling time with the corresponding deviation below 1 nV in the employed measurement configuration (see figure S2 in supplementary material).

## 3. Experimental results

### 3.1. Instability of molecular-doped epitaxial graphene in air

Epitaxial graphene doped by molecules in an organic matrix is unstable under ambient conditions. Figure 1 shows a typical magnetoresistance change in a graphene Hall device after 1 month of exposure to air in our laboratory. The laboratory maintained a temperature of 23 ± 0.1 °C and a relative humidity of 45 ± 5%. The initial longitudinal ($R_{xx}$) and Hall ($R_{xy}$) resistances are depicted by blue and red traces, respectively, while the final $R_{xx}$ and $R_{xy}$, measured over 1 month, are plotted by green and orange traces, respectively. We note that the charge carrier type is hole. The carrier type was determined by measuring the polarity of the Hall voltage according to the Lorentz force law. Two input terminals of the voltmeter were connected to Hall probes to lead a positive Hall

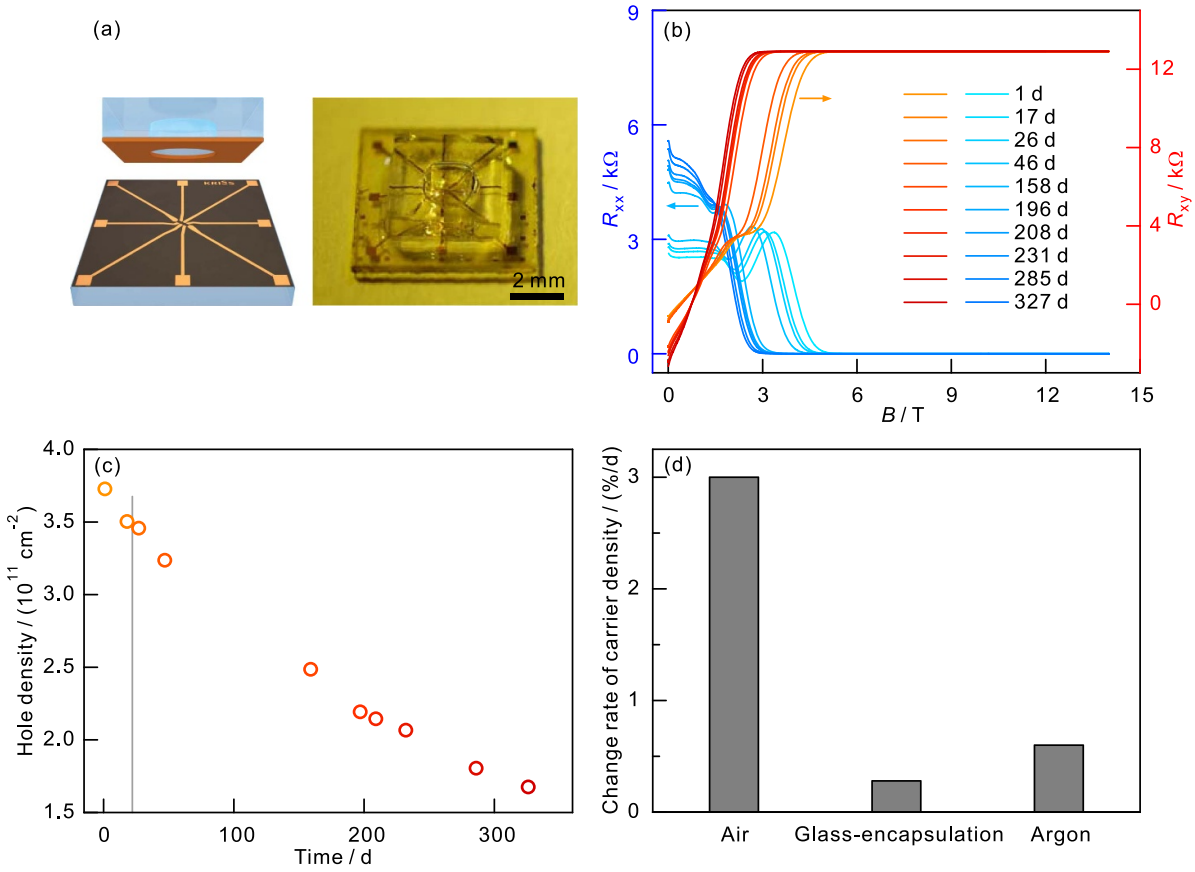


**Figure 2.** (a) Optical microscope image of the graphene Hall device with an illustration of a glass lid having a cavity at the center (left) and photograph of the graphene Hall device with the glass lid glued by an epoxy in a glove box (right). The orange layer underneath the glass lid denotes the applied epoxy. (b) Magnetoresistance measurements at 2 K through multiple thermal cycles over almost 1 year. (c) Time dependence of the hole density. The vertical gray line depicts 24 h exposure to 90% humidity for a robustness test. (d) Change rates of the carrier density in graphene devices stored in three different environments.

voltage. The Hall coefficient increased after exposure. This indicates a reduction in the hole density. In general, graphene becomes p-doped due to moisture or oxygen [44] through air exposure. The observed reduction in the hole density seems to be inconsistent with the general behavior of graphene in air. The reduction in the hole density might be attributed to a degradation of the dopant molecule (F4-TCNQ), arising from permeation of water or oxygen molecules through the polymer overlayer. The Hall quantization onset consequently begins at a smaller magnetic field. After air exposure, dissipation behavior was observed. The QHR significantly deviates from the nominal value of $R_K/2$, as depicted by the orange trace in the upper inset of figure 1. The deviation is larger than 4 Ω above the magnetic field of 5 T. The lower inset shows that the corresponding longitudinal resistance, plotted by the green trace, is larger than 1 Ω above the same magnetic field. We note that the initial quantization was confirmed with the CCC bridge, and the quantized resistance was close to the nominal value of $R_K/2$ within the measurement uncertainty of a few nΩ $\Omega^{-1}$. The observed dissipation behavior is attributed to disorders arising from air exposure. This control experiment clearly shows the instability of molecular-doped epitaxial graphene in air, which hinders convenient storage and delivery for metrological applications.

### 3.2. *Stability of glass-encapsulated molecular-doped epitaxial graphene*

We investigated the stability of a glass-encapsulated graphene device for almost 1 year. Figure 2(a) shows optical images of the graphene Hall device with a glass lid attached. Figure 2(b) shows how $R_{xx}$ and $R_{xy}$ change over time. The carrier density was extracted from the Hall resistance in the classical Hall regime. The carrier type is hole. We note that the encapsulated device was exposed to 90% humidity for 24 h between the 18th day and 27th day after device fabrication as a robustness test. The humidity exposure event is depicted by the vertical gray line in figure 2(c). The hole density decreases with time, as depicted in figure 2(c). The change rate has been decreasing with time, as shown in figure 2(c). For comparison, the carrier density change rates for an unencapsulated device (as shown in figure 1) and the glass-encapsulated device (as shown in figure 2(a)) are plotted together in figure 2(d). We note that the changing rate was extracted between carrier

densities of $2.5 \times 10^{11}$ cm$^{-2}$ and $3.0 \times 10^{11}$ cm$^{-2}$. The change rate of the encapsulated device is one order of magnitude smaller than that of the unencapsulated device. This change rate in the encapsulated device is comparable to that of an unencapsulated device, stored under an argon atmosphere at an approximate initial hole density of $2.5 \times 10^{11}$ cm$^{-2}$. Note that the observed magnetoresistance drift and carrier density change for almost 1 year were reproduced using another encapsulated device (see figure S3 in supplementary material).

Investigation of the microscopic origin of the carrier density change is beyond the scope of this work. Nevertheless, we consider the changing behavior qualitatively. The change in the carrier density in the glass-encapsulated graphene device or devices [34] stored under an inert gas may be attributed to either diffusion or degradation of dopants on graphene. The observed time dependence of the carrier density in the glass-encapsulated graphene device is not linear, while the Chalmers group reported a linear drift in the carrier density [34]. For a qualitative understanding, we tried to apply a simple diffusion model to the observed drift of the carrier density with time, as shown in figure 2(c). Details are described in figure S4 in the supplementary material.

To investigate the stability of the encapsulated device, we further performed precision measurements of the QHR at 4 K with the CCC bridge through multiple thermal cycles for almost 1 year. Figure 3(a) shows the Hall and longitudinal resistance measurements just after the 24 h humidity exposure. The relative difference between the measured Hall resistance and the nominal value of $R_K/2$ is depicted by the red hexagon as a function of the magnetic field. The corresponding longitudinal resistance is plotted by the blue dot. The lines are eye-guides. Good metrological quantization was achieved with a magnetic field exceeding 8 T. Unlike the unencapsulated device, the sizable deviation in $R_{xy}$ and the corresponding finite value in $R_{xx}$ were not observed. Figure 3(b) summarizes the measured quantization with time. We note that the on-set magnetic field for quantization decreased with time down to 6 T due to the reduction in the hole density, which is preferable for applications. Figure 3(c) exhibits the stability of the quantization at magnetic fields of 9 and 12 T. This indicates that the quantization does not change within the expanded measurement uncertainty of a few parts in $10^9$. The relative difference is comparable with the expanded measurement uncertainty. We note that a small deviation from the nominal value is observed as shown in figure 3, which might be attributed to a dissipation in the device near the charge neutrality or insufficient cooling [45] of the device in the employed cold-finger-type cryostat. We still cannot exclude a possible leakage current for the deviation due to a limited insulation of the employed probe. Note that the vertical gray line shows the 24 h humidity exposure.

We also investigated the robustness of Hall quantization with respect to the magnetic field and temperature after almost 1 year. Figure 4(a) shows the quantum Hall phase diagram for metrological criteria. Within the blue region, the relative deviation of the Hall resistance from $R_K/2$ is smaller than the expanded measurement uncertainty of 3 nΩ Ω$^{-1}$. Outside

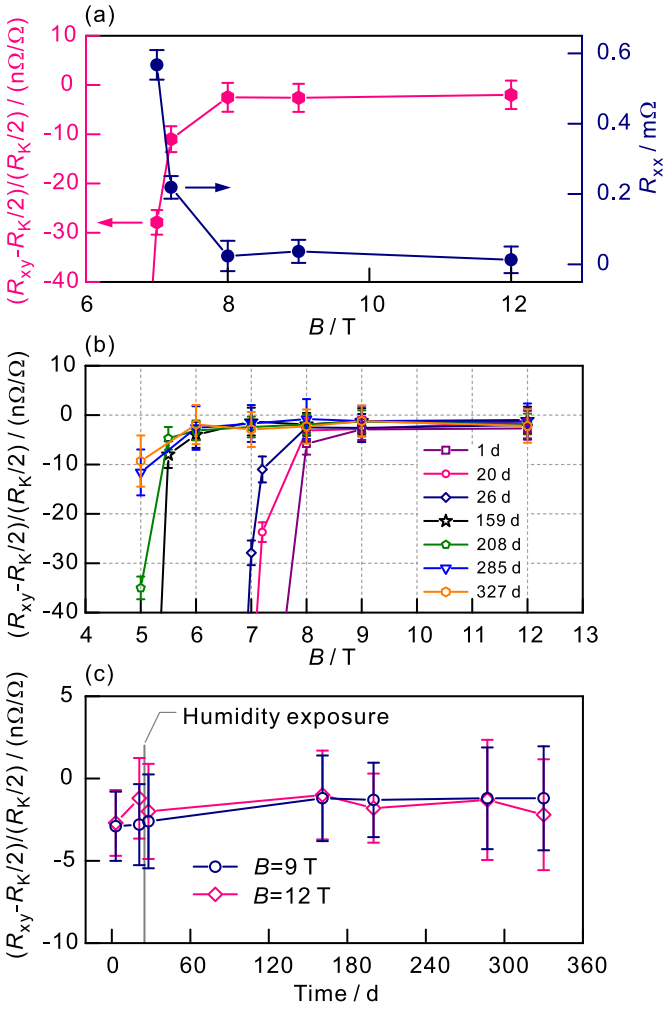


**Figure 3.** (a) Relative deviation of quantum Hall resistance at filling factor 2 from the nominal value of $R_K/2$ and the longitudinal resistance, depicted by the red hexagons and blue dots, respectively, as a function of the magnetic field. Error bars denote the expanded measurement uncertainty of $R_{xy}$ for the red hexagon or $R_{xx}$ for the blue dot. (b) Magnetic field dependence of the relative deviation plotted with respect to the number of days since device fabrication. (c) Stability of the Hall quantization at magnetic fields of 9 T and 12 T. The vertical gray line exhibits a 24 h exposure to 90% humidity for a robustness test.

of this region, depicted in red, the deviation and longitudinal resistance increase significantly by dissipation, which represents the breakdown of the quantum Hall state. Figures 4(b) and (c) show the relative deviation (depicted by the red hexagons) and longitudinal resistance (represented by the blue dots) with the temperature and the magnetic field fixed at 4 K and 8 T, respectively. Figure 4(b) shows that accurate Hall quantization can be achieved at 4 K and 6 T. From a practical point of view, it is important to realize the quantum resistance standard with a cryo-free system. We also note that the observed phase diagram is similar to that of a freshly fabricated graphene device with a similar initial carrier density. Regarding the critical current, the relative deviation of the Hall quantization from $R_K/2$ is smaller than 5 nΩ Ω$^{-1}$ with an applied current up to 80 μA at a magnetic field of 6 T.

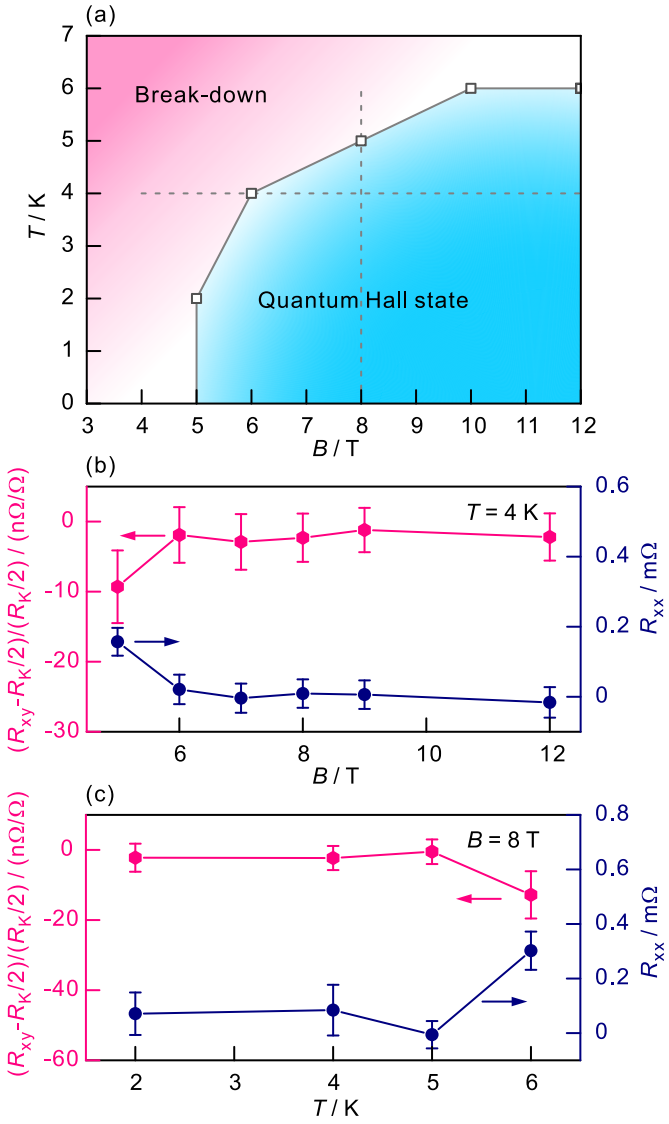


**Figure 4.** (a) Quantum Hall phase diagram for filling factor 2 as a function of the magnetic field and the temperature in the encapsulated graphene device after almost 1 year. (b) Relative deviation of the measured quantum Hall resistance from the nominal value (red hexagon) and longitudinal resistance (blue dot) at a fixed temperature of 4 K along the dotted horizontal line in (a). (c) Relative deviation of the measured quantum Hall resistance from the nominal value (red hexagon) and longitudinal resistance (blue dot) at a fixed magnetic field of 8 T along the dotted vertical line in (a). Error bars denote the expanded measurement uncertainty of $R_{xy}$ for the red hexagon or $R_{xx}$ for the blue dot.

## 4. Discussion

The employed molecule, F4-TCNQ, is widely used as a p-type dopant for graphitic materials [46–48]. However, the charge transfer state of F4-TCNQ on graphene and its stability are poorly understood from a microscopic point of view. For instance, the charge transfer state of F4-TCNQ in a conducting polymer matrix is unstable with time even in dark and inert gas environments [49]. Additionally, the conducting polymer becomes de-doped due to the oxygen molecules under ambient conditions rather than inert conditions [49]. The carrier density in molecular-doped epitaxial graphene near the charge neutrality under an argon atmosphere almost did not change (see figure S5 in supplementary material), while the carrier density in highly doped epitaxial graphene changed. The doping mechanism with F4-TCNQ and its long-term stability need to be investigated systematically by performing magnetoresistance measurements and infrared spectroscopy over time. Additionally, a further stability investigation will be performed with the presented device.

The carrier density of molecular-doped epitaxial graphene and its temporal stability are important parameters for the Hall quantization condition. Unlike the intact two-dimensional electron system at the interface of the GaAs–$Al_xGa_{1-x}As$ heterostructure, molecular-doped epitaxial graphene under ambient conditions is not stable owing to possible permeation of water and oxygen molecules through the polymer matrix or diffusion of dopant molecules in the polymer matrix. The lifetime of molecular-doped graphene devices for metrological applications was estimated according to the carrier density change rate [34]. We plotted the change rate with respect to the hole density for four devices (two glass-encapsulated devices and two bare graphene devices stored under argon) (see figure S6 in supplementary material). The change rate of the devices with an initial hole density on the order of $10^{11}$ $cm^{-2}$ decreases as the hole density decreases over time. This preliminary empirical relation is qualitatively consistent with the diffusion model, as suggested in figure S4. Note that the changing rate of a device, stored under argon, with an initial hole density below $10^{11}$ $cm^{-2}$ is approximately 0.04% per day, which is comparable to that of a previous result [34]. It is anticipated that the changing rate of a glass-encapsulated device would decrease further with time. If the observed drift, which is a reduction of the hole density, that is, an increase of the electron density, is maintained and an initial carrier density is close to the charge neutrality, the carrier type would change over time from hole to electron across the charge neutrality. To our knowledge, such bipolar temporal behavior in the given molecular-doped epitaxial graphene has not been reported. A further systematic investigation of the stability remains to be conducted to understand the above points.

We observed a small deviation of a few parts in $10^9$ from the nominal Hall quantization for filling factor 2 as shown in figures 3 and 4. To understand the origin of this deviation, we compared the Hall resistance measured in the ordinary orthogonal Hall configuration with that measured in a diagonal configuration containing the longitudinal resistance. Two measured Hall resistances were hardly distinguishable within the measurement uncertainty of approximately 3.5 nΩ $Ω^{-1}$. Nevertheless, we cannot exclude the possibility that dissipation, arising from inefficient cooling of the device with the employed cold-finger-type cryostat, may lead to a small deviation. We note that the wet environment is more efficient for device cooling than the dry environment, especially below the lambda point, as reported by Rigosi and his colleagues at the National Institute of Science and Technology, United States of America [45]. Additionally, we can conceive of

a leakage current through either the molecular dopant layer [34] or the semi-insulating SiC substrate for the small deviation, to be investigated. An insulation difference between a probe for GaAs-QHR standard at 0.3 K and the cold-finger-type cryostat for graphene-QHR at 2 K might introduce the observed deviation. We still cannot exclude the trivial quality of epitaxial graphene or disorders arising from the device-fabrication procedure for the observed deviation, requiring a systematic investigation with more devices. If QHR in graphene with a finite deviation is used as a quantum resistance standard in the future, the relevant error needs to be taken into account for the resistance measurement uncertainty budget.

## 5. Summary

In summary, the stability of glass-encapsulated molecular-doped epitaxial graphene was investigated for almost 1 year. Epitaxial graphene doped with F4-TCNQ was encapsulated with a glass lid to passivate molecular-doped epitaxial graphene against water and oxygen molecules in air. A glass-encapsulated device was stored under ambient conditions for the stability test. The carrier density and Hall quantization were monitored with time through multiple thermal cycles. The change rate of the carrier density in the glass-encapsulated device is one order of magnitude smaller than that of the control device without encapsulation. The observed change rate of the carrier density is comparable to that of the device stored under an inert argon atmosphere. The Hall quantization at filling factor 2 remains within the expanded measurement uncertainty of approximately 3.5 $n\Omega\ \Omega^{-1}$ even with changing carrier density over time. Experimental results suggest that classical glass encapsulation can be employed to minimize the carrier density change.

## Data availability statement

The data that support the findings of this study are available upon reasonable request from the authors.

## Acknowledgments

This research was supported by Research on Measurement Standards for Redefinition of SI Units funded by the Korea Research Institute of Standards and Science (Grant No. KRISS-2022-GP2022-0001). This work was supported in part by the Joint Research Project 18SIB07 GIQS (*Graphene Impedance Quantum Standard*) from the European Metrology Programme for Innovation and Research (EMPIR) co-financed by the Participating States and from the European Union's Horizon 2020 Research and Innovation Programme. In Korea, this collaborative project was supported by the National Research Foundation of Korea (Grant Nos. NRF-2019K1A3A1A78077479 and NRF-2021R1A2C4002128).

## ORCID iD

Dong-Hun Chae https://orcid.org/0000-0001-6394-9182

## References

[1] von Klitzing K, Dorda G and Pepper M 1980 New method for high-accuracy determination of the fine-structure constant based on quantized Hall resistance *Phys. Rev. Lett.* **45** 494
[2] Fletcher N, Rietveld G, Olthoff J, Budovsky I and Milton M 2014 Electrical units in new SI: saying goodbye to the 1990 values *NCSLI Meas. J. Meas. Sci.* **9** 30
[3] von Klitzing K 2017 Metrology in 2019 *Nat. Phys.* **13** 198
[4] Delahaye F and Jeckelmann B 2003 Revised technical guidelines for reliable dc measurements of the quantized Hall resistance *Metrologia* **40** 217
[5] Novoselov K S, Geim A K, Morozov S V, Jiang D, Zhang Y, Dubonos S V, Grigorieva I V and Firsov A A 2004 Electrical field effect in atomically thin carbon film *Science* **306** 666
[6] Novoselov K S, Geim A K, Morozov S V, Jiang D, Katsnelson M I, Grigorieva I V, Dubonos S V and Firsov A A 2005 Two-dimensional gas of massless Dirac fermion in graphene *Nature* **438** 197
[7] Zhang Y, Tan Y-W, Stormer H L and Kim P 2005 Experimental observation of the quantum Hall effect and Berry's phase in graphene *Nature* **438** 201
[8] Tzalenchuk A, Lara-Avila S, Kalaboukhov A, Paolillo S, Syväjärvi M, Yakimova R, Kazakova O, Janssen T J B M, Fal'ko V and Kubatkin S 2010 Towards a quantum resistance standard based on epitaxial graphene *Nat. Nanotechnol.* **5** 186
[9] Ribeiro-Palau R *et al* 2015 Quantum Hall resistance standard in graphene devices under relaxed experimental conditions *Nat. Nanotechnol.* **10** 965
[10] Janssen T J B M, Rozhko S, Antonov I, Tzalenchuk A, Williams J M, Melhem Z, He H, Lara-Avila S, Kubatkin S and Yakimova R 2015 Operation of graphene quantum Hall resistance standard in a cryogen-free table-top system *2D Mater.* **2** 035015
[11] Kruskopf M *et al* 2016 Comeback of epitaxial graphene for electronics: large-area growth of bilayer-free graphene on SiC *2D Mater.* **3** 041002
[12] Yang Y *et al* 2017 Epitaxial graphene homogeneity and quantum Hall effect in millimeter-scale devices *Carbon* **115** 229
[13] Park J, Kim W-S and Chae D-H 2020 Realization of 5 with graphene quantum Hall resistance array *Appl. Phys. Lett.* **116** 093102
[14] Riedl C, Coletti C, Iwasaki T, Zakharov A A and Starke U 2009 Quasi-free-standing epitaxial graphene on SiC obtained by hydrogen intercalation *Phys. Rev. Lett.* **103** 246804
[15] Kopylov S, Tzalenchuk A, Kubatkin S and Fal'ko V I 2010 Charge transfer between epitaxial graphene and silicon carbide *Appl. Phys. Lett.* **97** 112109
[16] Kalmbach C-C, Schurr J, Ahlers F J, Müller A, Novikov S, Lebedeva N and Satrapinski A 2014 Towards a graphene-based quantum impedance standard *Appl. Phys. Lett.* **105** 073511
[17] Schurr J, Kalmbach C-C, Ahlers F J, Hohls F, Kruskopf M, Müller A, Pierz K, Bergsten T and Haug R J 2017 Magnetocapacitance and dissipation factor of epitaxial graphene-based quantum Hall effect devices *Phys. Rev.* B **96** 155443

[18] Kruskopf M *et al* 2020 Graphene quantum Hall effect devices for AC and DC electrical metrology *IEEE Trans. Electron Devices* **68** 3672

[19] Ristein J, Mammadov S and Seyller T 2012 Origin of doping in quasi-free-standing graphene on silicon carbide *Phys. Rev. Lett.* **108** 246104

[20] Lara-Avila S, Moth-Poulsen K, Yakimova R, Bjørnholm T, Fal'ko V, Tzalenchuk A and Kubatkin S 2011 Non-volatile photochemical gating of an epitaxial graphene/polymer heterostructure *Adv. Mater.* **23** 878

[21] Lartsev A, Yager T, Bergsten T, Tzalenchuk A, Janssen T J B M, Yakimova R, Lara-Avila S and Kubatkin S 2014 Tuning carrier density across Dirac point in epitaxial graphene on SiC by corona discharge *Appl. Phys. Lett.* **105** 063106

[22] Yang Y, Huang L-I, Fukuyama Y, Liu F-H, Real M A, Barbaba P, Liang C-T, Newell D B and Elmquist R E 2015 Low carrier density epitaxial graphene devices on SiC *Small* **11** 90

[23] He H *et al* 2018 Uniform doping of graphene close to the Dirac point by polymer-assisted assembly of molecular dopants *Nat. Commun.* **9** 3956

[24] Li D, Borkent E-J, Nortrup R, Moon H, Katz H and Bao Z 2005 Humidity effect on electrical performance of organic thin-film transistors *Appl. Phys. Lett.* **86** 042105

[25] Grossiord N, Kroon J M, Andriessen R and Blom P W M 2012 Degradation mechanisms in organic photovoltaic devices *Org. Electron.* **13** 432

[26] Cui Z 2016 *Printed Electronics: Materials, Technologies and Applications* (Hoboken, NJ: Wiley and Higher Education Press)

[27] Yazdi G R, Akhtar F, Ivanov I G, Schmidt S, Shtepliuk I, Zakharov A, Iakimov T and Yakimova R 2019 Effect of epitaxial graphene morphology on adsorption of ambient species *Appl. Surf. Sci.* **486** 239

[28] Rigosi A F *et al* 2018 Examining epitaxial graphene surface conductivity and quantum Hall device stability with parylene passivation *Microelectron. Eng.* **194** 51

[29] Rigosi A F, Liu C-I, Glavin N R, Yang Y, Hill H M, Hu J, Walker A R H, Richter C A, Elmquist R E and Newell D B 2017 Electrical stabilization of surface resistivity in epitaxial graphene systems by amorphous boron nitride encapsulation *ACS Omega* **2** 2326

[30] Rigosi A F *et al* 2017 Preservation of surface conductivity and dielectric loss tangent in large-scale, encapsulated epitaxial graphene measured by noncontact microwave cavity perturbation *Small* **13** 1700452

[31] Sarkar S, Zhang H, Huang J-W, Wang F, Bekyarova E, Lau C N and Haddon R C 2013 Organometallic hexahapto functionalization of single layer graphene as a route to high mobility graphene devices *Adv. Mater.* **25** 1131

[32] Che S, Jasuja K, Behura S K, Nguyen P, Sreeprasad T S and Berry V 2017 Retained carrier-mobility and enhanced plasmonic-photovoltaics of graphene via ring-centered functionalization and nanointerfacing *Nano. Lett.* **17** 4381

[33] Rigosi A F *et al* 2019 Gateless and reversible carrier density tenability in epitaxial graphene devices functionalized with chromium tricarbonyl *Carbon* **142** 468

[34] He H *et al* 2019 Polymer-encapsulated molecular doped epigraphene for quantum resistance metrology *Metrologia* **56** 045004

[35] Chae D-H *et al* 2021 Investigation of the stability of graphene devices for quantum resistance metrology at direct and alternating current *Meas. Sci. Technol.* **33** 065012

[36] Burrows P E, Bulovic V, Forrest S R, Sapochak L S, McCarty D M and Thompson M E 1994 Reliability and degradation of organic light emitting devices *Appl. Phys. Lett.* **65** 2922

[37] Emtsev K V *et al* 2009 Towards wafer-size graphene layers by atmospheric pressure graphitization of silicon carbide *Nat. Mater.* **8** 203

[38] Xia F, Perebeinos V, Lin Y-M, Wu Y and Avouris P 2011 The origins and limits of metal-graphene junction resistance *Nat. Nanotechnol.* **6** 179

[39] Rikken G L J A, van Haaren J A M M, van der Wel W, van Gelder A P, van Kempen H, Wyder P, André J P, Ploog K and Weimann G 1988 Two-terminal resistance of quantum Hall devices *Phy. Rev.* B **37** 6181

[40] Part No. 63017 'Epoxy Quickset' from UHU GmbH, Buehl, Germany We cured the epoxy in a glove box at room temperature for 24 h

[41] Gournay P, Rolland B, Chae D-H and Kim W-S 2020 On-site comparison of quantum Hall effect resistance standards of the KRISS and the BIPM: ongoing key comparison BIPM.EM-K12 *Metrol. Tech. Suppl.* **57** 01010

[42] Drung D, Götz M, Pesel E, Storm J-H, Aßmann C, Peters M and Schurig T 2009 Improving the stability of cryogenic current comparator setups *Supercond. Sci. Technol.* **22** 114004

[43] Drung D, Götz M, Pesel E and Scherer H 2015 Improving the traceable measurement and generation of small direct currents *IEEE Trans. Instrum. Meas.* **64** 3021

[44] Liu H, Liu Y and Zhu D 2011 Chemical doping of graphene *J. Mater. Chem.* **21** 3335

[45] Rigosi A F *et al* 2019 Graphene devices for tabletop and high-current quantized Hall resistance standards *IEEE Trans. Instrum. Meas.* **68** 1870

[46] Chen W, Chen S, Qi D C, Gao X Y and Wee A T S 2007 Surface transfer p-type doping of epitaxial graphene *J. Am. Chem. Soc.* **129** 10418

[47] Coletti C, Riedl C, Lee D S, Krauss B, Patthey L, von Klitzing K, Smet J H and Starke U 2010 Charge neutrality and band-gap tuning of epitaxial graphene on SiC by molecular doping *Phy. Rev.* B **81** 235401

[48] Park J *et al* 2012 Single-gate bandgap opening of bilayer graphene by dual molecular doping *Adv. Mater.* **24** 407

[49] Watts K E, Neelamraju B, Ratcliff E L and Pemberton J E 2019 Stability of charge transfer states in $F_4$TCNQ-doped P3HT *Chem. Mater.* **31** 6986